DOI: 10.1002/ejic.200500414

The Ligation Properties of some Reduced Schiff Base Selena/Telluraaza Macrocycles: Versatile Structural Trends

Snigdha Panda,[a] Sanjio S. Zade,[a] Harakesh B. Singh,*[a] and Ray J. Butcher[b]

Keywords: Chalcogenaaza macrocycles / Selenium tellurium ligands / Nickel / Palladium / Platinum

The chalcogenaaza macrocycles **4**, **5** and **6** show versatility in ligation properties towards various transition metal ions. The structure of the reduced 22-membered selenaaza macrocycle **4** ($C_{32}H_{36}N_4Se_2$) has been determined. The Ni^{II} complex **7** exhibits coordination by the N4Se2 donor sites. The Pd^{II} complexes **8**, **9**, **10**, and **14** have been structurally characterized. The molecular structures of these complexes reveal interesting versatile ligating behaviors of the ligands. The Pd complexes **8**, **9**, and **14** display coordination by hard nitrogen donor atoms only, whereas the complex **10** showed coordination by N2Te2 donor centers. The Pt^{II} complex **11** shows the formation of a cationic metallamacrocycle with C–Pt–Se linkage. The crystal structures suggest that the coordination of metal atoms to donors is determined by the geometrical arrangement around the metal and by the conformation of the macrocycle rather than by the HSAB (hard/soft acid/base) principle.

Introduction

The mixed donor macrocycles have attracted considerable interest due to their high selective nature for complexation of ions. Amongst the chalcogenaaza macrocycles, oxaaza and thiaaza have been well studied[1] relative to their heavier counterparts. Incorporation of the larger Se and Te would lead to a change in the size of the cage cavity and hence allow for some interesting coordination behavior. There are only a few reports on homodonor selenium- and tellurium-containing macrocycles and their ligating behavior towards the metal ions.[2,3] Only recently, some mixed donor macrocycles incorporating selenium and tellurium have been reported.[4–7]

As part of our research on the design and synthesis of heavier chalcogenaaza macrocycles, we recently reported the synthesis and complexation studies of the selenaaza and telluraaza Schiff base macrocycles **1**–**3**.[5–7] However, these Schiff base macrocycles are prone to transmetallation and hydrolysis on treatment with metal salts, which leads to cleavage of the macrocycle. The selenaaza Schiff base macrocycle **1** forms the hydrolyzed product with the Pd^{II} cation,[7] whereas the telluraaza Schiff base macrocycle **2** forms transmetallated products with Pt^{II} and Hg^{II} cations.[5] The hydrolysis of the selenaaza macrocycle **1** may be due to excessive strain on the ring, which is forced by the metal to adopt a planar geometry. The facile cleavage of the C–Te bond in **2** is due to strong N→Te intramolecular interactions, which activate the *trans* C–Te bond. This strong intramolecular interaction is mainly due to the presence of the sp^2 nitrogen atom. To synthesize stable complexes of chalcogenaaza macrocycles, we are now interested in the ligation behavior of the reduced forms of the Schiff base macrocycles **4**–**6**. The reduced forms of the macrocycles are more flexible. Also these macrocycles have only sp^3 hybridized atoms and can accommodate a larger range of shapes and sizes than the Schiff base macrocycles that have sp^2 hybridized donor atoms. In the reduced forms, the macrocycles have weaker E···N (E = Se, Te) interactions as evidenced from the multinuclear NMR spectra and single-crystal X-ray structures (vide infra). We reported, in a preliminary communication, the ligation properties of **4** and **5** with Pd^{II} and Pt^{II}.[8] It was found that the macrocycle **4** forms a 23-membered metallamacrocycle on ligation with Pt^{II}, in which a C–Se bond is oxidatively added to the Pt^{II} center to form a hexacoordinate Pt^{IV} complex (**11**). Complexes **8** and **10** show contrasting ligation behavior of the macrocycles **4** and **5** with Pd^{II}. In **8**, the coordination sites are hard nitrogen donors only, whereas in **10** the coordination sites are occupied by N2Te2. In this paper, we now report a systematic study of the ligation properties of the reduced selena/telluraaza macrocycles with transition metal ions. The ligation properties of the reduced selenaaza macrocycle **4** with a series of transition metal cations (Ni^{II}, Pd^{II}, Pt^{II} Cu^{II}, and Hg^{II}), the ligation properties of the telluraaza macrocycle **5** with Pd^{II}, and the ligation properties of the 28-membered selenaaza macrocycle **6** with Pd^{II} have been investigated.

[a] Department of Chemistry, Indian Institute of Technology Bombay,
Powai, Mumbai, 400076, India
E-mail: chhbsia@chem.iitb.ac.in
[b] Department of Chemistry, Howard University,
Washington, D. C. 20059, USA

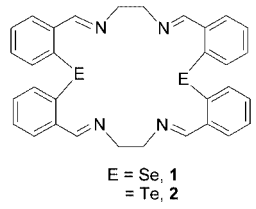

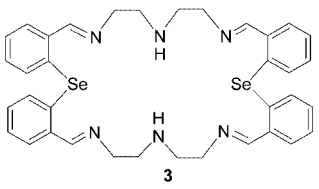

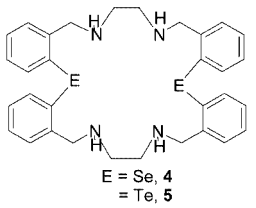

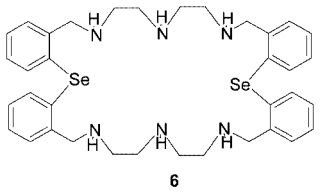

Result and Discussion

The ligands **4**–**6** were prepared by following known procedures.[5–7] The molecular structure of the ligand **4** (Figure 1, Table 1) is centrosymmetric, and only half of the molecule represents the asymmetric unit. The structure confirms the complete reduction of the Schiff base macrocycle. Of two possible nitrogen atoms available for interaction, only one interacts weakly with the Se atom. The Se···N(1A) distance (3.01 Å) is shorter than the sum of the van der Waals radii of Se (1.99 Å) and N (1.53 Å). The transannular Se···Se distance (4.75 Å) is longer than the Se···Se distance (3.808 Å) in the parent Schiff base **1**.[7] The geometry around Se is V-shaped. The C(1B)–Se–C(1A) bond angle is 98.04°, which is smaller than that in the parent Schiff base (100.2°). The macrocycle framework is puckered so as to suit the bonding pattern of the individual atoms.

Table 1. Significant bond lengths [Å] and angles [°] for **4**.

Se–C(1A)	1.926(2)	Se–C(1B)	1.938(3)
N(1A)–C(8A)	1.459(3)	N(1A)–C(7A)	1.464(3)
N(1B)–C(8B)	1.460(3)	N(1B)–C(7B)	1.475(3)
C(1A)–Se–C(1B)	98.03(10)	C(8A)–N(1A)–C(7A)	113.1(2)
C(8B)–N(1B)–C(7B)	114.0(2)	C(2A)–C(1A)–Se	120.6(2)
C(6A)–C(1A)–Se	119.16(18)	N(1A)–C(7A)–C(6A)	111.1(2)
C(6B)–C(1B)–Se	120.95(19)	N(1B)–C(7B)–C(6B)	117.1(2)
N(1B)–C(8B)–C(8A)#	1110.6(2)		

Equimolar amounts of **4** and $Ni(OCOCH_3)_2$ in MeOH were heated to reflux for 30 min, and subsequent addition of NH_4PF_6 yielded a purple complex **7**, which was crystallized by slow diffusion of diethyl ether into the acetonitrile solution of the complex at room temperature (Scheme 1). The complex was soluble in MeCN, $MeNO_2$, acetone, DMSO, and DMF, and stable in air. The elemental analysis data of the complex suggest the formation of the 1:1 product. The molecular ion peak was not observed in the FAB mass spectrum of the complex, however, there are peaks centered at m/z = 838 for M – PF_6 and at m/z = 693 for M – $2PF_6$. The IR spectrum shows peaks at 840 and 557 cm^{-1} corresponding to ν(P–F) and ν(F–P–F), respectively. The solution phase electronic spectrum (>200 nm) of the complex consists of three bands centered at 304 (ε = 2400 $dm^3 mol^{-1} cm^{-1}$), 699 (15 $dm^3 mol^{-1} cm^{-1}$), and 895 nm (29 $dm^3 mol^{-1} cm^{-1}$). The solid-state absorption spectrum of the complex exhibits the same type of bands centered at 316, 564, and 894 nm. This indicates that the complex is stable in solution and in the solid state and has the same structure in both states. The μ_{eff} (B.M.) is 3.39, which is larger than the value usually observed. Larger values are

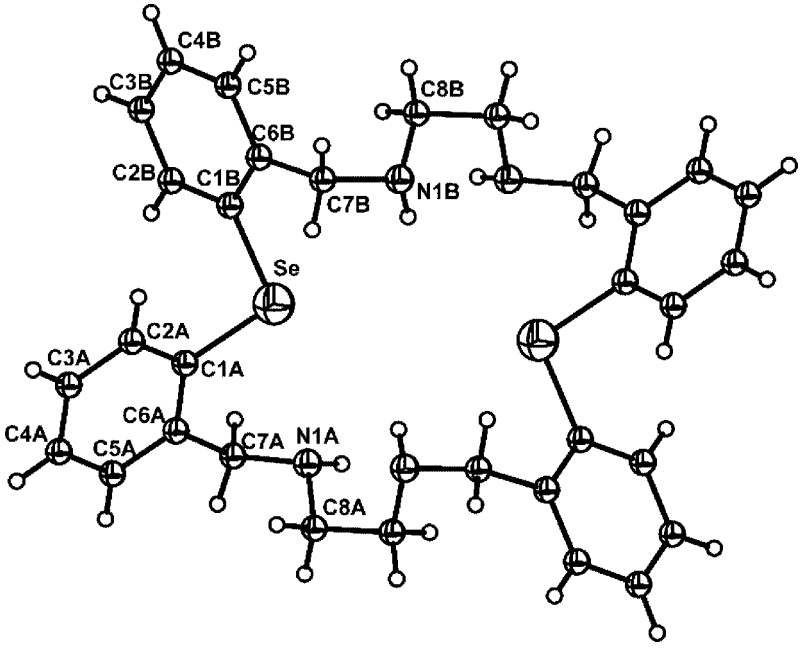

Figure 1. ORTEP diagram of the ligand **4**.

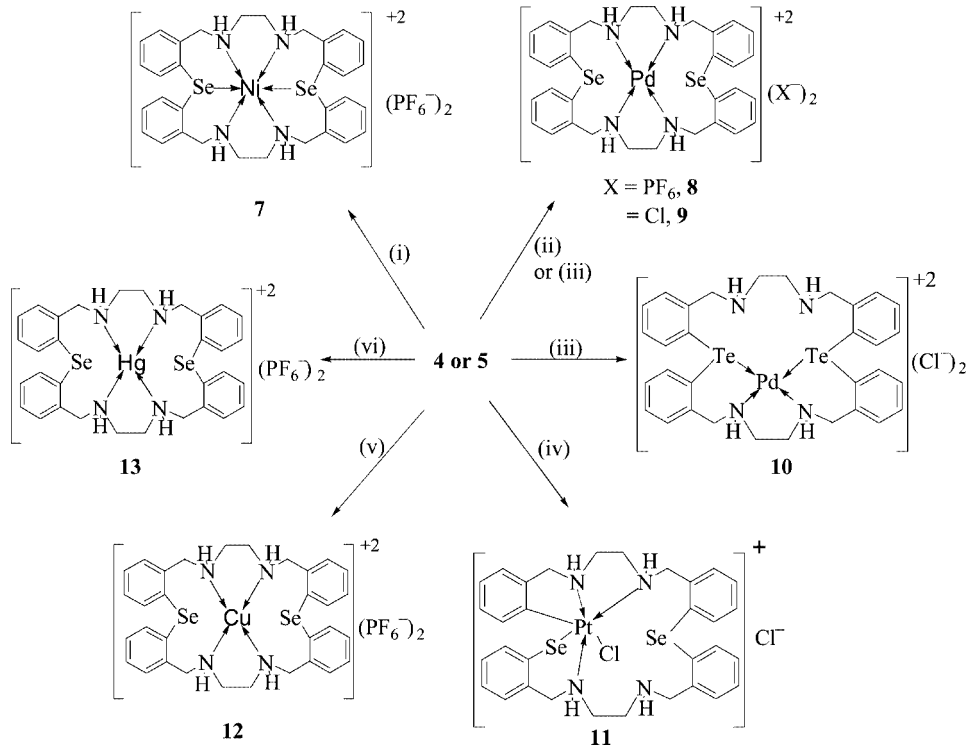

Scheme 1. Reagents: MeOH (reflux), (i) $Ni(OCOCH_3)_2$, NH_4PF_6; (ii) $Pd(C_6H_5CN)_2Cl_2$, NH_4PF_6; (iii) $PdCl_2$, (iv) $PtCl_2$; (v) $Cu(CH_3CN)_4ClO_4$, NH_4PF_6; (vi) $Hg(OCOCH_3)_2$, NH_4PF_6.

generally observed as a result of orbital contributions derived from the mixing of low-lying excited states into the ground state or because the ground state is orbitally degenerate. As expected for octahedral Ni^{II} complexes, complex **7** is EPR silent.[9,10] The cyclic voltammogram of the Ni^{II} complex **7** shows a quasi-reversible oxidation peak at –0.211 V and a reduction peak at –0.092 V. There is a substantial shift to a more negative potential on changing from imine to amine nitrogen donors,[7] as expected, given that this change results in a reduction of π-acceptor ability.[11]

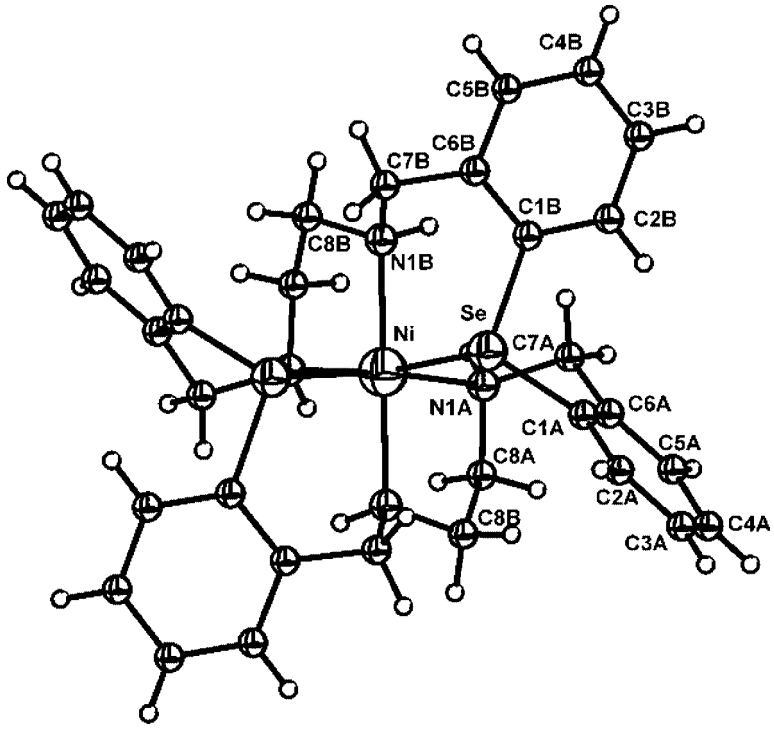

Figure 2. ORTEP diagram for **7**.

There are very few reports on the molecular structures of Ni complexes of selenium-containing macrocycles. This is the third example of the molecular structure of a nickel complex with a selenium-containing macrocycle.[7] The molecular structure (Figure 2, Table 2) is centrosymmetric and is similar to that of the Ni^{II} complex of the parent ligand. The structure shows that the Ni^{II} ion occupies the macrocyclic cavity and is bonded to all four nitrogen and two selenium donors of the macrocycle thus adopting an octahedral geometry. The bond lengths are: Ni–N(1B) 2.104(2) Å, Ni–N(2B) 2.104(2), Ni–N(1A) 2.115(2), Ni–N(2A) 2.115(2), Ni–Se 2.6189(4) Å. The Ni–Se bond length is comparable to Ni–Se distances in *trans*-[$NiCl_2$(Me-$SeCH_2CH_2SeMe_2$)][12] and is also comparable to that observed for the parent Schiff base Ni complex.[7] The C–Se–C bond angle is 101.73(10)°, which is larger than that of the parent Schiff base Ni complex [97.1(7)°]. The two Se atoms are *cis* to each other in the distorted octahedral geometry as they are in the parent Schiff base Ni complex.

Table 2. Significant bond lengths [Å] and angles [°] for **7**.

Ni–N(1B)	2.104(2)	Ni–N(1A)	2.115(2)
Ni–Se	2.6189(4)		
N(1B)#1–Ni–N(1B)	173.22(12)	N(1B)–Ni–N(1A)#1	83.53(8)
N(1B)–Ni–N(1A)	91.81(8)	N(1A)#1–Ni–N(1A)	93.54(12)
N(1B)#1–Ni–Se	96.36(6)	N(1B)–Ni–Se	88.74(5)
N(1A)#1–Ni–Se	170.30(6)	N(1A)–Ni–Se	92.56(6)
Se–Ni–Se#1	82.435(18)		

The corresponding palladium complexes **8** and **9** were obtained by the reaction of $Pd(C_6H_5CN)_2Cl_2$ and $PdCl_2$, respectively, with 1 mol of ligand **4** in refluxing methanol, followed by the addition of excess NH_4PF_6 in the case of **8** (Scheme 1). The complexes are soluble only in DMSO. The elemental analysis data suggest the formation of a 1:1 complex. The crystals were grown from DMSO/ether. The peaks at 843 and 558 cm^{-1} in the IR spectrum confirms the presence of a PF_6^- ion. The molecular ion peak of complex **8** is not observed in its FAB mass spectrum; peaks at *m*/*z* = 886 and 735 correspond to M – PF_6 and M – 2 PF_6, respectively. The ESI-MS spectrum of **9** exhibits a peak at *m*/*z* = 840, which corresponds to M + $2H_2O$, and a peak at *m*/*z* = 741, which corresponds to M – 2Cl. The ^{1}H- and ^{13}C NMR spectra for both **8** and **9** are too complicated for complete analysis. The ^{77}Se NMR spectra of **8** and **9** display peaks at 869 and 787 ppm, respectively. As the ^{77}Se NMR spectra of both complexes exhibit single signals, which were shifted downfield relative to that of the free ligand (δ = 329 ppm), it is possible that metal coordination to selenium occurs in solution. Variable-temperature ^{1}H NMR spectroscopy was carried out on **8** at higher temperatures (20 °C–120 °C) in DMSO solution (Figure 3). As the temperature was increased, line broadening resulted in the coalescence of the peaks. Upon cooling to room temperature, the original spectrum was restored. The coalescence phenomena of the spectra may occur as a result of the fluxional behavior of the complex in solution. The only fluxional process that achieves this result is one in which the metal effectively hops between the six donor sites of the macrocycle, as illustrated in Scheme 2. This hopping of the Pd^{II} center between the N4Se2 coordination sites is similar to that reported by McAuley et al.,[13] where, in a square-planar palladium complex, the Pd^{II} center hops between any four of the six donor sites. However, an N3Se coordination is ruled out, since the ^{77}Se NMR spectrum shows a single peak. The ^{1}H NMR spectra at ambient and high temperatures do not exhibit any resonances that could be assigned to the free ligand in solution, which suggests that the interconversion does not proceed though a dissociative mechanism.

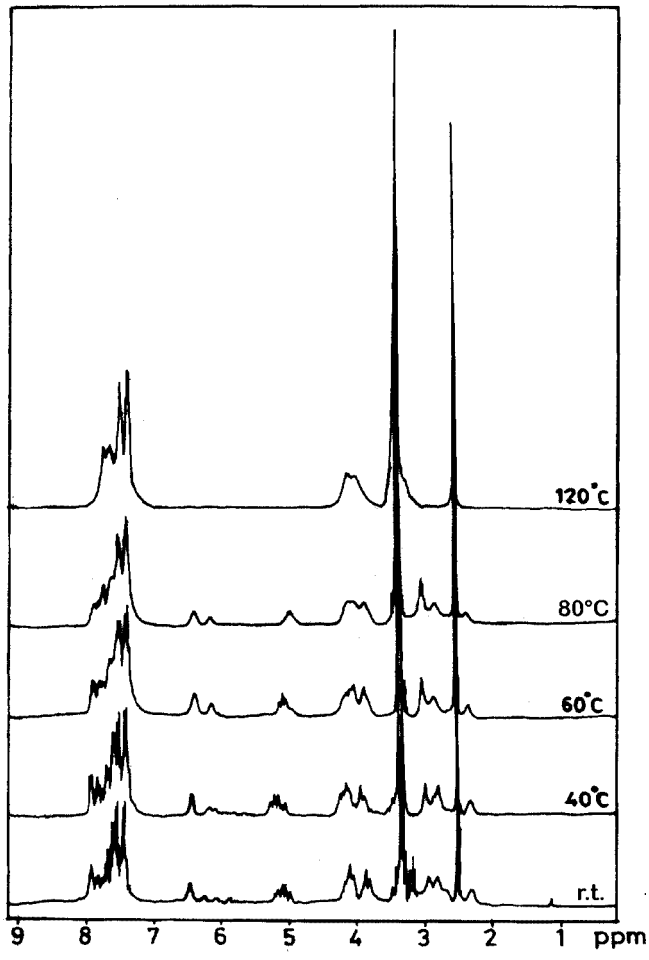

Figure 3. Variable-temperature ^{1}H NMR ([D_6]DMSO, 300 MHz) spectra of **8**.

Since complexes **8** and **9** are isostructural (Figure 4, Figure 5, Table 3, Table 4), the crystal structure of only **8** will be discussed, and major differences between the structures will be highlighted. Both structures are centrosymmetric like the parent macrocycle **4**, and only half of the molecule represents the asymmetric unit. The cation adopts a square-planar geometry and is coordinated to the four nitrogen atoms. The N–Pd–N bond angles are ca. 180° and ca. 90°. The Pd–N bond lengths are in good agreement with the sum of the single-bond covalent radii of Pd (1.31 Å) and N (0.75 Å).[14] However, these bond lengths are slightly longer than that observed for the hydrolyzed parent Schiff base [2.019(6) Å],[7] which has sp^2 hybridized N donor atoms. In the solid-state molecular structures, the palladium atom

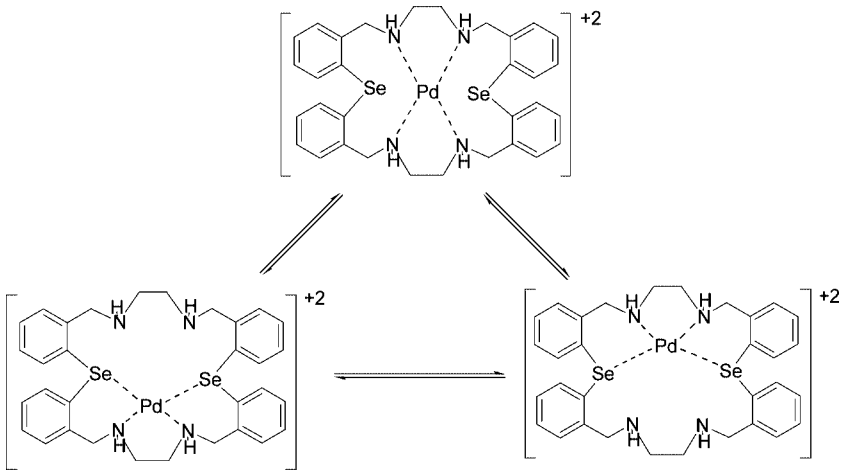

Scheme 2. Fluxional process for **8** in solution.

does not coordinate to the Se atom. This is in contrast to the solid-state structures of Pd^{II} complexes of the mixed donor Se/Te macrocycles that contain O or P, in which Pd^{II} coordinates to the soft Se/Te donor centers.[4] This anomalous behavior may be due to the formation of stable five-membered chelate rings rather than to the formation of six-membered chelate rings that would result in coordination to the Se donors. In this case, the absence of any interaction between the Se and Pd^{II} atoms probably results from the conformational requirement of the ligand around the central Pd^{II} atom for coordination with donor atoms, as well as the chelate ring effect. Complex **9** crystallizes with two waters of crystallization; however, there is no hydrogen bonding between the water molecules and the chloride counterions. The transannular Se···Se bond length of **8** is 9.310 Å and that of **9** is 9.670 Å.

Equimolar amounts of **5** and $PdCl_2$ in MeOH were heated to reflux for 15 min to yield a clear solution of the complex **10**; brown crystals were obtained by slow diffusion of diethyl ether into the reaction mixture at room temperature (Scheme 1). Complex **10** is not very soluble in CH_3CN and CH_3NO_2 but highly soluble in DMSO. The elemental analysis data confirm the formation of a 1:1 complex. The molecular ion peak of complex **10** is not observed in its ESI

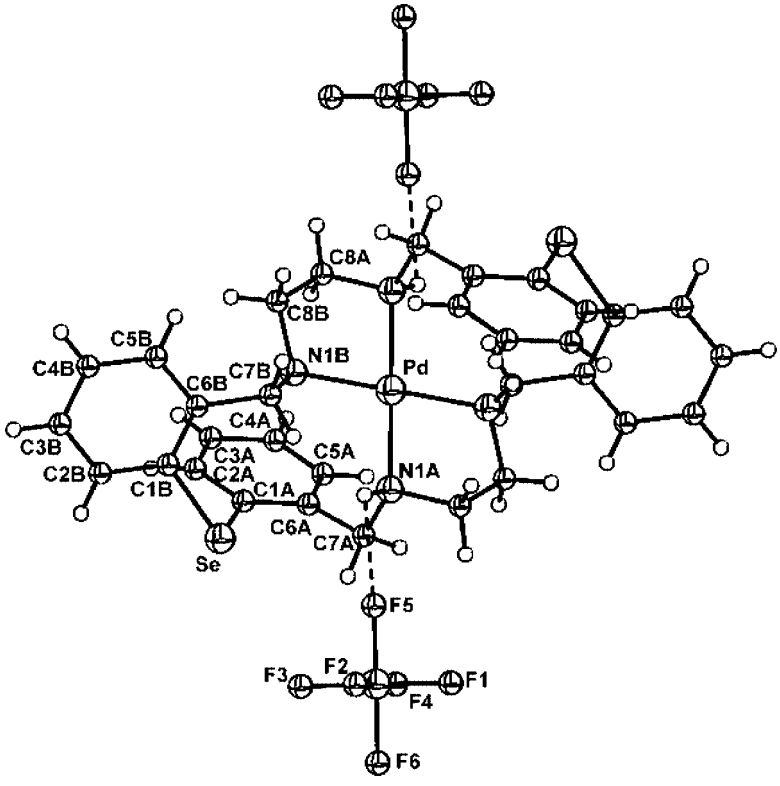

Figure 4. ORTEP diagram for **8**.

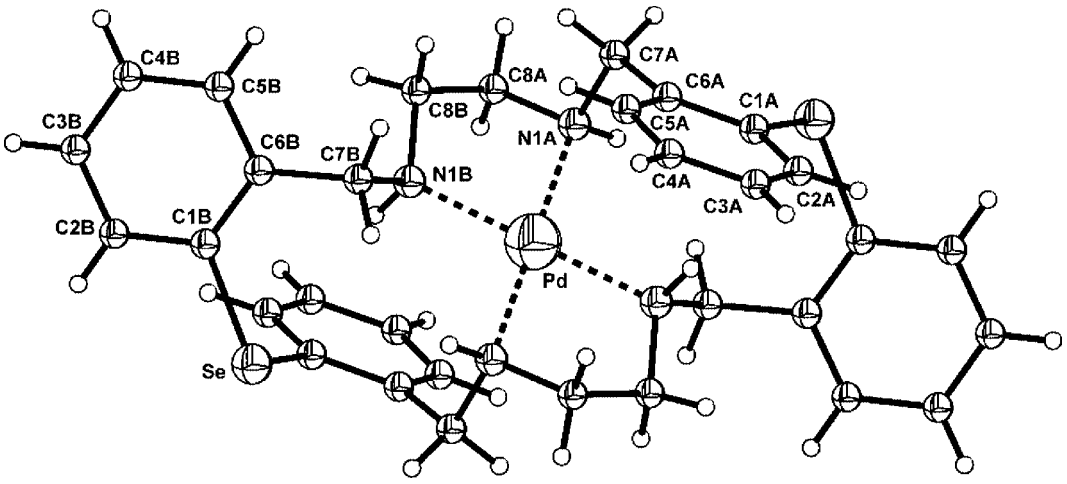

Figure 5. ORTEP diagram of **9**.

Table 3. Significant bond lengths [Å] angles [°] for **8**.

Pd–N(1B)	2.063(2)	Pd–N(1A)	2.066(3)
N(1B)–Pd–N(1B)#1	180.000(1)	N(1B)–Pd–N(1A)#1	83.73(10)
N(1B)#1–Pd–N(1A)#1	96.27(10)	N(1B)–Pd–N(1A)	96.27(10)

Table 4. Significant bond lengths [Å] and angles [°] for **9**.

Pd–N(1)	2.072(4)	Pd–N(2)	2.060(5)
N(2)#1–Pd–N(2)	180.0(2)	N(2)#1–Pd–N(1)	96.90(18)
N(2)–Pd–N(1)	83.10(18)		

mass spectrum; the highest peak at m/z = 838 corresponds to the M – 2Cl fragment. The ^{125}Te NMR spectrum of complex **10** in [D_6]DMSO shows a peak at δ = 710 ppm, which disappeared after half an hour due to decomposition of the complex. A complex pattern of signals that were difficult to assign was observed in the ^{1}H and ^{13}C NMR spectra.

An ORTEP diagram of compound **10** is shown in Figure 6, and selected bond lengths and angles are given in Table 5. The molecule crystallizes with seven waters of crystallization. The Pd^{II} cation adopts a square-planar geometry and is coordinated to the two nitrogen and two tellurium atoms. The tellurium atoms are slightly disordered. The Pd–N(1A) [2.114(6) Å] and Pd–N(2A) [2.118(8) Å] are slightly longer than the sum of the single bond covalent radii of Pd (1.31 Å) and N (0.75 Å).[14] However, these bond lengths are well within the sum of van der Waals radii. The Te–Pd bond lengths [Te(1A)–Pd 2.5770(16) Å, Te(2A)–Pd 2.5675(12) Å, Pd–Te(1B) 2.480(7) Å, and Te(2B)–Pd 2.431(4) Å] are significantly shorter than the sum of covalent radii (2.68 Å) and are comparable to those in the parent Schiff base macrocycle Pd complex.[5] The N–Pd–N, Te–Pd–Te, and N–Pd–Te bond angles are close to 90° and 180°. The coordination to Te in **10** may be due to the greater σ-donor property of the Te than Se, which leads to a stronger soft–soft interaction and stabilization of the six-membered chelate ring. The packing diagram (Figure 7) shows that the water molecules are sandwiched between the complexes and that there is extensive hydrogen bonding between the N–H hydrogen atom, chloride counterion, and the water molecules.

Equimolar amounts of **4** and $PtCl_2$ in MeOH were heated to reflux for 15 min to yield a clear solution of the complex **11**; brick-red crystals were obtained by slow diffusion of diethyl ether into the reaction mixture at room temperature (Scheme 1). The complex formed was not very soluble in most of the organic solvents and only partially soluble in MeOH. The elemental analysis data suggest the formation of a 1:1 complex. The molecular ion peak of complex **11** is absent in its ESI mass spectrum; the highest peak observed at m/z = 863 corresponds to M – (Cl + 2 H_2O). The ^{1}H and ^{13}C NMR spectra of complex **11** are too complicated for complete analysis. As complex **11** is only partially soluble in MeOH, no satisfactory ^{77}Se NMR spectrum could be recorded even after overnight data acquisition.

The X-ray crystal structure of **11** (Figure 8, Table 6) clearly suggests the formation of a novel 23-membered metallamacrocyclic complex. The geometry around Pt^{IV} is octahedral.[8] The Pt–N bond *trans* to Pt–Se is longer (ca. 0.15 Å) than the other two Pt–N bonds because of the strong *trans* influence of –SePh.[15] The Pt–C bond length [2.010(4) Å] is shorter than those of the reported Pt^{IV} selenolate compounds,[15–17] whereas the Pt–Cl bond length [2.4291(12) Å] is longer than those in related compounds.[16] This lengthening of the Pt–Cl bond and the shortening of the C–Pt bond may be ascribed to the stronger *trans* influence of phenyl ring than of Cl. The behavior of the macrocycle to form the cationic Pt^{IV} complex by oxidative addition of the C–Se bond to the Pt^{II} center is in contrast to those of the reported stable Pt^{II} and Pt^{IV} complexes with homodonor and mixed donor cyclic selenoether ligands.[4,18] The facile oxidative addition in this case may be facilitated by the more polar nature of C–Se bond that results from the N→Se intramolecular interaction present in the parent macrocycle (vide supra). Though the oxidative addition of halogens and alkyl halides to the Pt^{II} center are

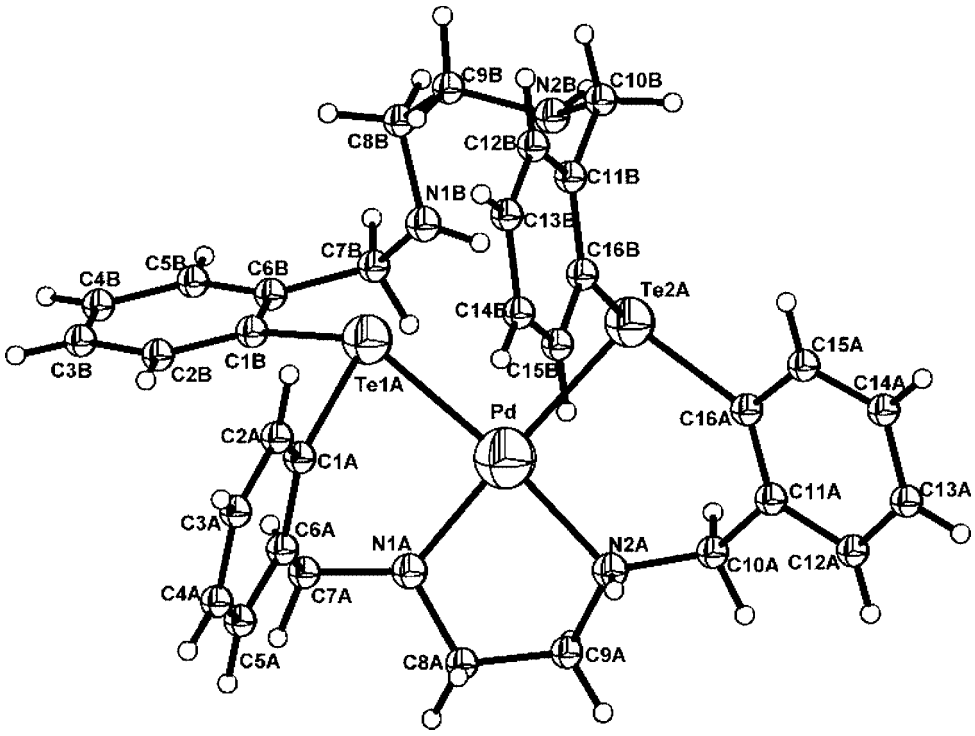

Figure 6. ORTEP diagram of **10**.

Table 5. Significant bond lengths [Å] and angles [°] for **10**.

Te(1A)–Pd	2.5770(16)	Te(2A)–Pd	2.5675(12)
Pd–Te(1B)	2.480(7)	Pd–Te(2B)	2.431(4)
Pd–N(1A)	2.114(6)	Pd–N(2A)	2.118(8)
Te(1A)–Pd–Te(2A)	89.67(5)	N(1A)–Pd–Te(1A)	94.34(18)
N(1A)–Pd–N(2A)	83.9(3)	N(2A)–Pd–Te(2A)	94.0(2)
N(2A)–Pd–Te(1A)	164.18(19)	N(1A)–Pd–Te(2A)	172.18(18)

common,[19] this is the second example of oxidative addition of C–Se bond to Pt^{II}.

Complex **12** was obtained by the reaction of $Cu(CH_3CN)_4ClO_4$ with 1 mol of ligand **4** in refluxing methanol, followed by the addition of excess NH_4PF_6. The complex is soluble in DMSO, MeCN, and $MeNO_2$. The crystals obtained from DMSO lose luster after removal of the solvent.

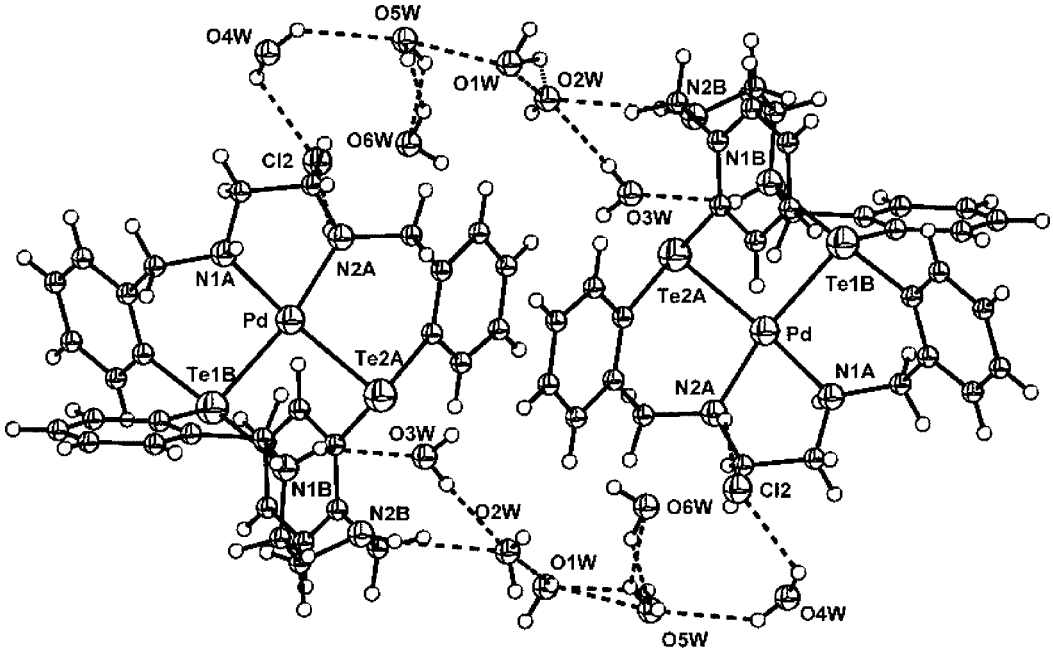

Figure 7. Packing diagram of **10**.

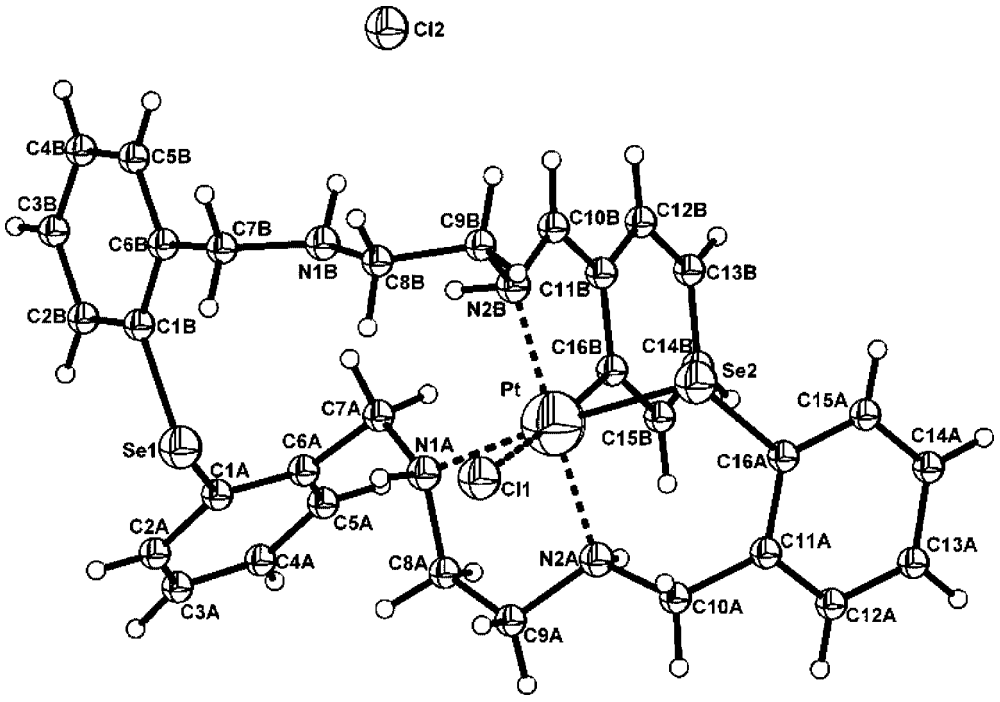

Figure 8. ORTEP diagram of **11**.

Table 6. Significant bond lengths [Å] and angles [°] for **11**.

Pt–C(16B)	2.010(4)	Pt–N(2B)	2.039(4)
Pt–N(2A)	2.050(4)	Pt–N(1A)	2.180(3)
Pt–Se(2)	2.4165(6)	Pt–Cl(1)	2.4291(12)
Se(1)–C(1A)	1.917(4)	Se(1)–C(1B)	1.924(5)
Se(2)–C(16A)	1.897(5)		
C(16B)–Pt–Se(2)	88.53(11)	C(16B)–Pt–N(2B)	81.51(17)
N(2A)–Pt–Se(2)	93.87(9)	N(2A)–Pt–N(1A)	82.37(12)
N(2B)–Pt–N(1A)	97.26(13)		

The elemental analysis data confirm the formation of a 1:1 complex. Complex **12** was found to be a 1:2 electrolyte in acetonitrile ($\Lambda_{M,}$ 393 $\Omega^{-1}\,cm^2\,mol^{-1}$). The infrared spectrum of the complex exhibits two NH stretching vibrations at 3301 and 3235 cm^{-1} as sharp singlets and a bending vibration at 1629 cm^{-1} as a broad singlet, while the IR spectrum of the ligand shows the stretching vibrations at 2794–3323 cm^{-1} (sharp multiplets) and the bending vibration at 1687 cm^{-1}(sharp singlet). This implies that N–H of the ligand is involved in coordination to the metal center. The peaks at 843 and 557 cm^{-1} confirm the presence of PF_6 in the complex. The solution-phase electronic spectrum (>200 nm) of the complex consists of two intense bands centered at 298 (ε = 2485 $dm^3\,mol^{-1}\,cm^{-1}$) and 583 nm (148 $dm^3\,mol^{-1}\,cm^{-1}$), which can be assigned to the intraligand π–π* transitions. The reflectance spectrum of the solid sample exhibits the same type of bands centered at 315 and 584 nm. This indicates that the complex is stable in solution. The observed magnetic susceptibility value for the complex is 1.79 BM. This value is close to that for the square-planar copper complexes (1.84 BM).[20] The electron spin resonance spectrum further confirms the square-planar geometry of the complex. The spectrum of the powdered form is not well resolved; however, at the temperature for liquid nitrogen, an anisotropic ESR spectrum is obtained. The spectrum exhibits a line shape that is typical for a mononuclear Cu^{II} complex with a $d_{x^2-y^2}$ ground state. The $g_\perp$ value for the complex is 2.052. The value for $A_\parallel$ was calculated from the difference between the peak positions i.e. 180G. The g_z value is 2.24. This g_z value is greater than that of $g_\perp$. The anisotropic value for g_x and g_y has not been resolved and no $A_\perp$ hyperfine constant was observed. The quotient $(g_z \times 10^4)/A_\parallel$ is an indication of the stereochemistry of the chelates in solution.[21] It has been suggested that this quotient may be an empirical index of tetrahedral distortion from tetragonal geometry, i.e. values that are lower than 140 are observed for square-planar structures and those that are higher than 150 for tetrahedral complexes. A value of 124 for **12** indicates a square-planar geometry. The Cu^{II} complexes of tetraaza macrocyclic ligands generally exhibit irreversible redox processes. The Cu^{II} complex **12** is reduced directly to Cu^0 by a single two-electron process at –0.524 V. Such behavior may stem from the higher flexibility of the ligand, which does not allow the Cu^I complex to be kinetically stable and enables the reduction of the Cu^{II} center directly to Cu^0.[22]

The reaction of $HgCl_2$ with ligand **4** gave an insoluble white product, which was not soluble in any of the common solvents. However, when the reaction was performed with $Hg(OCOCH_3)_2$, a white product **13** was obtained, which is soluble in MeCN and $MeNO_2$, and decomposes in DMSO. The elemental analysis data suggest the formation of a 1:1 complex. The IR spectrum shows a broad multiplet in the region of NH stretching (2911–3671 cm^{-1}). The peaks at 841 and 558 cm^{-1} correspond to ν(P–F) and ν(F–P–F), respectively. The molecular ion peak of complex **13** is not

observed in the ESI mass spectrum, as is the case for the other complexes; the peak observed at m/z = 981 is assigned to M – PF_6, and the peak at m/z = 834 corresponds to M – 2 PF_6. This indicates the formation of the complex with two PF_6 counterions, and the peak at m/z = 635 shows that the macrocycle remains intact. The broadening of the ^{1}H NMR signal in the aliphatic region indicates the presence of molecular motion, which is somewhat slow on the NMR time scale. The existence of isomeric species in solution is also a possibility. The ^{13}C NMR shows the expected number of peaks. The ^{77}Se NMR spectrum exhibits a single signal at δ = 315 ppm, which indicates that there is no interaction between Se and Hg^{II}. The Hg^{II} complex **13** shows two irreversible reduction peaks at 0.505 and 0.032 V, which implies the sequential reduction of Hg^{II} to Hg^{I} and then to Hg^0.

Reaction of ligand **6** with 1 and 2 equiv. Pd(COD)Cl_2, followed by the addition of NH_4PF_6 afforded the complexes **14** and **15** in a 1:1 and 1:2 (ligand/metal) ratio, respectively (Scheme 3).

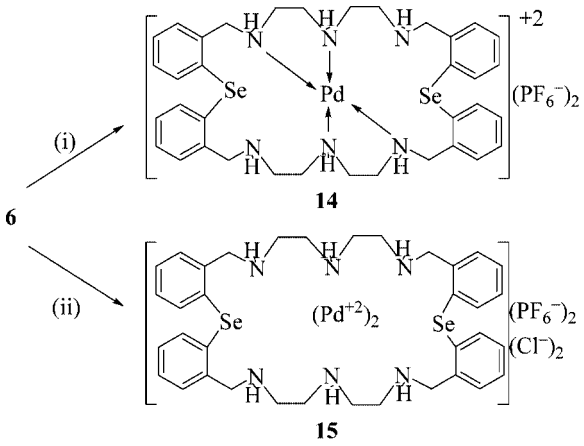

Scheme 3. Reagents: MeOH (reflux), (i) **6**:Pd(COD)Cl_2 (1:1), NH_4PF_6; (ii) **6**:Pd(COD)Cl_2 (1:2), NH_4PF_6.

Complex **14** is light yellow, whereas complex **15** is yellow. The complexes are not very soluble in all solvents even on prolonged heating. Due to the partial solubility of the complexes, complete characterization of the complexes was difficult. The elemental analysis data for **14** and **15** suggest the formation of 1:1 and 1:2 (ligand/metal) complexes respectively. The IR spectra exhibit peaks in the range 840–849 and at 556 cm^{-1}, which correspond to ν(P–F) and ν(F–P–F), respectively. In the ESI mass spectrum of complex **14**, the molecular ion peak is observed at m/z = 1116.88, and the peaks for [M – PF_6], [M – 2 PF_6], and [M – (Pd + 2 PF_6)] are observed at m/z = 971.9, 826.9, and 719, respectively. However, for complex **15**, no molecular ion peak is observed; peaks at m/z = 1148.96, 1112.95, 1075.95, and 928.98 are observed for [M – PF_6], [M – (PF_6 + Cl)], [M – (PF_6 + 2 Cl)], and [M – 2 (PF_6 + Cl)]. Due to the poor solubility of complexes, it was challenging to record the ^{77}Se NMR spectrum of the complexes. The ^{77}Se NMR spectrum of complex **14** was recorded in 50% CD_3CN/CD_3OD solution and shows one peak at δ = 303 ppm after long data accumulation. However, the ^{77}Se NMR spectrum of compound **15** could not be recorded. The Pd^{II} complexes did not show well-defined redox processes that could be interpreted.

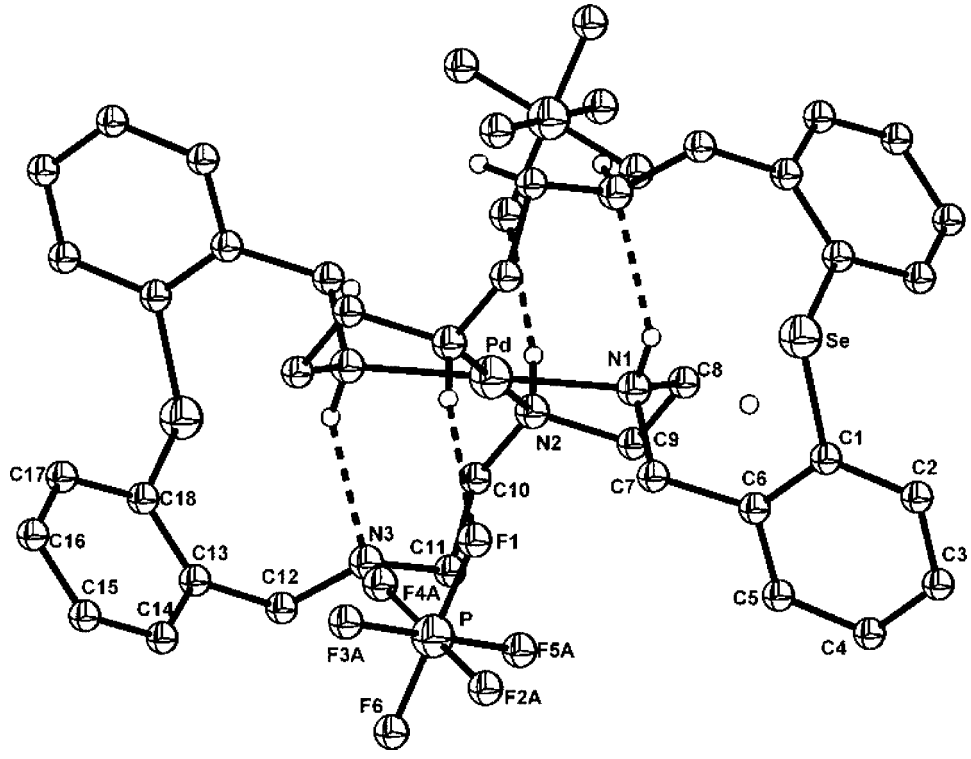

Figure 9. ORTEP diagram of **14**.

The ORTEP view of compound **14** is shown in the Figure 9, and selected bond lengths and angles are given in the Table 7. The molecule is centrosymmetric: only half of the molecule represents the asymmetric unit, and there is one molecule per unit cell. The cation adopts a square-planar geometry and coordinates to four nitrogen atoms out of the possible N6Se2 coordination sites. The N(1)–Pd–N(1)# and N(2)–Pd–N(2)# bond angles are 180°. The N(1)–Pd–N(2) bond angle is 84.05(13)°, and these atoms are part of a five-membered ring containing two nitrogen donor atoms. The N(1)–Pd–N(2)#1 bond angle is 95.95(13)°, and these atoms are part of a 13-membered ring containing an Se atom. The Pd–N(1) and Pd–N(2) bond lengths are 2.067(3) and 2.081(3) Å, respectively, and are marginally longer than the sum of the covalent radii of Pd (1.31 Å) and N (0.75 Å); however, they are much shorter than the sum of the van der Waals radii. The phenyl rings and the two selenium atoms bend away from the square plane that contains the Pd cation. The transannular distance between the two Se atoms is 10.422 Å.

Table 7. Significant bond lengths [Å] angles [°] for **14**.

Pd–N(1)	2.067(3)	Pd–N(2)	2.081(3)
N(1)–Pd–N(1)#1	180.0	N(1)–Pd–N(2)	84.05(13)
N(1)#1–Pd–N(2)	95.95(13)		

The synthesis of the Pt^{II} analogues of **14** and **15** has been attempted. Though elemental analysis, and IR and ESI mass spectrometry show the formation of the desired complexes, no satisfactory NMR spectra could be obtained because of the highly insoluble nature of the complexes. Attempts to get suitable crystals were also unsuccessful.

Conclusions

In conclusion, macrocycle **4** shows versatile coordination behavior towards the metal cations Ni^{II}, Pd^{II}, Pt^{II}, Cu^{II}, and Hg^{II}. In general, molecular structures of the complexes show that the coordination behavior of the metal ions towards the donors is determined by the geometrical arrangement of the ligands around the metal atom, by the stability of the chelate ring formed by metal coordination, and to a lesser extent, by the HSAB principle.

Experimental Section

General: All reactions were carried out under nitrogen or argon using standard vacuum line techniques. Solvents were purified and dried by standard procedures[23] and were freshly distilled prior to use. Melting points were recorded in capillary tubes and are uncorrected. The ^1H (299.4), ^{13}C (75.42), and ^{77}Se (57.22) NMR spectra were recorded in [D_6]DMSO or CD_3CN on a Varian VXR 300S spectrometer. Chemical shifts cited were referenced to TMS (^1H, ^{13}C) as internal and Me_2Se (^{77}Se) as external standards. The elemental analysis was performed on a Carlo–Erba model 1106 and Eager 300 EA1112 elemental analyzers. The IR spectra were recorded as KBr pellets with a Thermo Nicolet Avatar 320 FTIR spectrometer. The UV/Vis spectra in solution were recorded with 3-cm path length quartz cells on a UV-260 Shimadzu spectrophotometer, and reflectance spectra were recorded with a UV-160A spectrophotometer. The electronic spectra of all the complexes were recorded at room temperature in acetonitrile. The spectra were recorded in the range 200–1100 nm. The FAB mass spectra were recorded on a JEOL SX 102/DA-6000 mass spectrometer/data system using Argon/Xenon (6 KV, 10 mA) as the FAB gas. The ESI mass spectra were recorded at room temperature with a Q-Tof micro (YA-105) micromass spectrometer. The magnetic susceptibility of the complexes **7** and **12** was studied at room temperature. Complex $Hg[Co(SCN)_4]$ was used as the standard. The EPR spectra were recorded at room temperature and at the temperature for liquid nitrogen. TCNQ was taken as the standard. $Cu(CH_3CN)_4ClO_4$, $Pd(C_6H_5CN)_2Cl_2$, and $Pd(COD)Cl_2$ were prepared by literature procedures.[24] All the complexes were vacuum dried after preparation. The solution electrical conductivity was measured using a Elico CM-180 Conductivity meter with KCl solution in water as standard. Cyclic voltammetric (CV) experiments were performed on a CH instruments electrochemical analyzer with a three-electrode device. The experiments were performed with a glassy carbon working electrode, a platinum counter electrode, and a standard Ag/AgCl reference electrode. Tetrabutylammonium perchlorate (Aldrich) was used as the supporting electrolyte. All solutions were purged with nitrogen before the CV data were recorded. Measurements were recorded with 0.1 M NBu_4ClO_4 in acetonitrile with a sample concentration 0.05 mM. Ferrocene was taken as the standard.

Syntheses

Ligands **4**, **5**, and **6** were prepared following known procedures.[6,7]

[$NiC_{32}H_{36}N_4Se_2P_2F_{12}$] (7): $Ni(OCOCH_3)_2$ (0.026 g, 0.15 mmol) was added to ligand **4** (0.1 g, 0.15 mmol) in methanol (20 cm^3). The reaction mixture was then heated to reflux for 30 min. The resulting reaction mixture was filtered, and to the filtrate excess NH_4PF_6 was added to give the complex as a purple powder. Crystallization from an acetonitrile solution by diffusion of diethyl ether afforded purple crystals of the complex. Yield: 0.078 g, 52%. M.p. 269 °C (d.). Magnetic susceptibility: 3.39μ_B. IR (KBr): $\tilde{\nu}_{max}$ = 3286 (m), 2923 (s), 1641 (b), 1461 (m), 1308 (w), 1083 (m), 951 (w), 840 (s), 760 (s), 557 (s) cm^{-1}. λ_{max} (MeCN; ε/$dm^3 mol^{-1} cm^{-1}$): 304 (2400), 699 (15) and 895 (29) nm. FAB MS: *m*/*z* = 839 [M – PF_6], 693 [M – 2 PF_6]. $C_{32}H_{36}N_4Se_2NiP_2F_{12}$ (983.2): calcd. C 39.09, H 3.69, N 5.69; found C 38.41, H 3.60, N 7.05.

[$PdC_{32}H_{36}N_4Se_2P_2F_{12}$] (8):[8] Complex **8** was prepared in a manner similar to that of **7**, but with the metal precursor $Pd(C_6H_5CN)_2Cl_2$. Cream-coloured crystals were obtained from a DMSO/ether solution. Yield: 0.087 g, 56%. M.p. 247–249 °C (d.). IR (KBr): $\tilde{\nu}_{max}$ = 3426 (b), 3220 (m), 2924 (w), 1631 (w), 1449 (m), 1020 (w), 843 (s), 764 (s), 558 (s) cm^{-1}. ^{77}Se NMR ([D_6]DMSO): δ = 869 ppm. FAB MS: *m*/*z* = 886 [M – PF_6], 738 [M – 2 PF_6]. $C_{32}H_{36}N_4Se_2PdP_2F_{12}$: calcd. C 37.28, H 3.52, N 5.43; found C 36.88, H 3.68, N, 5.02.

[$C_{32}H_{40}Cl_2N_4O_2PdSe_2$] (9): $PdCl_2$ (0.027 g, 0.15 mmol) was added to **4** (0.1 g, 0.15 mmol) in MeOH (20 cm^3), and heated to reflux for 30 min. The reaction mixture was filtered. The solvent volume was reduced to 2 cm^3 in vacuo, followed by diffusion of diethyl ether to afford yellowish crystals of the complex. Yield: 0.075 g, 61%. M.p. 225 °C (d.). IR (KBr): $\tilde{\nu}_{max}$ = 3426 (s), 3226 (s), 3052 (m), 2849 (s), 1632 (s), 1464 (s), 1440 (s), 1340 (w), 1199 (w), 1025 (s), 755 (s), 633 (w), 452 (w) cm^{-1}. ^{77}Se ([D_6]DMSO): δ = 787 ppm. ESI-MS: *m*/*z* = 840 [M + 2 H_2O], 741 [M – 2 Cl]. $C_{32}H_{40}Cl_2N_4O_2PdSe_2$ (847.9): calcd. C 45.34, H 4.76, N 6.61; found C 45.58, H 5.05, N 6.27.

[$PdC_{32}H_{36}N_4Te_2Cl_2$] (10):[8] This complex was prepared in a manner similar to that described for **9** and was isolated as brownish red crystals from a methanol/ether solution. Yield: 0.2 g, 78%. M.p. 196 °C (d.). IR (KBr): $\tilde{\nu}_{max}$ = 3417 (s, br), 3320 (s), 3049 (m), 2881 (s), 2850 (s), 1621 (m), 1439 (s), 1205 (m), 1120 (m), 837 (s), 752 (s) cm^{-1}. ESI-MS: *m*/*z* = 838 [M – 2 Cl]. $C_{32}H_{36}N_4Te_2PdCl_2H_2O$: calcd. C 41.45, H 4.13, N 6.04; found C 40.88, H 4.22, N 5.77.

[$PtC_{32}H_{40}N_4O_2Se_2Cl_2$] (11):[8] This complex was prepared in a manner similar to that described for **9** and was isolated as red crystals by the slow diffusion of diethyl ether. Yield: 0.074 g, 52%. M.p. 252 °C (d.). IR (KBr) $\tilde{\nu}_{max}$ = 3429 (br), 2923 (s), 2848 (s), 1635 (s), 1439 (s), 1327 (s), 1105 (w), 1026 (s), 751 (s) cm^{-1}. ESI-MS: 863.2 [M – Cl], 827.21 [M – 2 Cl]. $C_{32}H_{40}N_4O_2Se_2PtCl_2$: calcd. C 41.05, H 4.30, N 5.98; found C 41.93, H 3.46, N 6.41.

[$CuC_{32}H_{36}N_4Se_2P_2F_{12}$] (12): This complex was prepared by following the method used for preparing complex **7** but with $Cu(CH_3CN)_4ClO_4$. Yield: 0.050 g, 33%. M.p. 212–214 °C (d.). Magnetic susceptibility: 1.79μ_B. IR (KBr): $\tilde{\nu}_{max}$ = 3434 (m), 3301 (s), 2941 (w), 1629 (w), 1465 (s), 1347 (w), 1302 (w), 1199 (w), 1106 (m), 1042 (m), 927 (s), 843 (s), 622 (s), 760 (s), 577 (s) cm^{-1}. λ_{max} (MeCN; ε/$dm^3\,mol^{-1}\,cm^{-1}$): 298 (2485), 583 (148). Molar conductivity (acetonitrile, 298 K): Λ_M = 393 $\Omega^{-1}\,cm^2\,mol^{-1}$. FAB MS: *m*/*z* = 697 [M – 2 PF_6], 637 [M – (2 PF_6 + Cu)]. $C_{32}H_{36}N_4Se_2CuP_2F_{12}$ (988.1): calcd. C 38.90, H 3.67, N 5.67; found C 39.38, H 3.87, N 6.27.

[$HgC_{32}H_{36}N_4Se_2P_2F_{12}$] (13): This complex was prepared in a manner similar to that described for **7** but with the metal precursor $Hg(OCOCH_3)_2$. Yield: 0.066 g, 38%. M.p. 180 °C (d.). IR (KBr): $\tilde{\nu}_{max}$ = 3671 (w), 3271 (w), 2928 (w), 1587 (w), 1461 (s), 1439 (s), 1204 (w), 1018 (w), 841 (s), 760 (s), 558 (s) cm^{-1}. ^{13}C NMR (CD_3CN): δ = 47.1 (CH_2NH), 54.3 (CH_2Ar), 129.6, 131.3, 131.6, 135.2, 136.9 (Aromatic C) ppm. ^{77}Se NMR (CD_3CN): δ = 315 ppm. ESI-MS: *m*/*z* = 981 [M – PF_6], 835 [M – 2 PF_6]. $C_{32}H_{36}N_4Se_2HgP_2F_{12}$ (1125.1): calcd. C 34.16, H 3.22, N 4.98; found C 33.93, H 3.31, N 4.86.

[$PdC_{36}H_{46}N_6Se_2P_2F_{12}$] (14): Pd(COD)$Cl_2$ (0.057 g, 0.2 mmol) was added to **6** (0.15 g, 0.2 mmol) in MeOH (20 cm^3) and was heated to reflux for 30 min. The reaction mixture was filtered, and to the filtrate excess NH_4PF_6 was added. The solvent volume was reduced to 2 cm^3 in vacuo, followed diffusion of diethyl ether to afford colorless crystals. Yield: 0.15 g, 32%. M.p. 220 °C (d.). IR (KBr): $\tilde{\nu}_{max}$ = 3343 (br), 3236 (s), 2927 (br), 840 (s), 557 (s) cm^{-1}. ^{77}Se NMR

Table 8. Crystal data and structure refinement of **4**, **7**, **8**, and **9**.

	4	**7**	**8**	**9**
Empirical formula	$C_{32}H_{36}N_4Se_2$	$C_{32}H_{36}F_{12}N_4P_2NiSe_2$	$C_{32}H_{46}F_{12}N_4P_2PdSe_2$	$C_{32}H_{40}Cl_2N_4O_2Pd\ Se_2$
M_w	635.7	983.22	1030.91	847.90
Crystal system	Monoclinic	Tetragonal	Triclinic	Monoclinic
Space group	P2/*n*	P4(2)/*n*	$P\bar{1}$	*P*21/*n*
a [Å]	16.3985(14)	15.5381(8)	9.9501(14)	11.4547(18)
b [Å]	5.0714(4)	15.5381(8)	10.5010(15)	11.4404(18)
c [Å]	18.2454(15)	15.2794(15)	10.6403(16)	12.864(2)
α [°]	90	90	103.622(2)	90
β [°]	104.4830(10)	90	117.296(2)	95.428(3)
γ [°]	90	90	103.042(3)	90
V [Å^3]	1469.1(2)	3688.9(5)	885.6(2)	1678.2(5)
Z	2	4	1	2
Temperature [K]	293(2)	168(2)	168(2)	103(2)
Abs. coeff. [mm^{-1}]	2.544	2.678	2.765	2.917
Observed reflections [$I > 2\sigma$]	3581	4501	5787	4083
Final *R*(F) [$I > 2\sigma$][a]	0.0416	0.0297	0.0330	0.0688
wR(F_2) indices [$I > 2\sigma$]	0.0669	0.0568	0.0442	0.1462

[a] $R(F_o) = \Sigma||F_o| - |F_c||/\Sigma|F_o|$ and $wR(F_o^2) = [\Sigma w(F_o^2 - F_c^2)^2/\Sigma w(F_c^2)^2]^{1/2}$.

Table 9. Crystal data and structure refinement of **10**, **11**, and **14**.

	10	**11**	**14**
Empirical formula	$C_{32}H_{50}Cl_2N_4O_7PdTe_2$	$C_{32}H_{39}Cl_2N_4O_2Pt\ Se_2$	$C_{36}H_{46}F_{12}N_6P_2PdSe_2$
M_w	1035.26	935.58	1117.05
Crystal system	Triclinic	Triclinic	Triclinic
Space group	$P\bar{1}$	$P\bar{1}$	$P\bar{1}$
a [Å]	12.072(6)	9.9635(19)	10.3868(1)
b [Å]	13.264(6)	10.210(2)	10.4193(1)
c [Å]	14.527(7)	17.427(3)	10.9246(1)
α [°]	104.235(8)	94.196(3)	108.532(1)
β [°]	107.668(9)	105.466(3)	95.200(1)
γ [°]	110.244(8)	106.808(4)	108.573(1)
V [Å^3]	1912.6(16)	1613.7(5)	1038.110(17)
Z	2	2	1
Temperature [K]	293(2)	103(2)	294(2)
Abs. coeff. [mm^{-1}]	2.169	6.806	7.152
Observed reflections [$I > 2\sigma$]	8797	7802	3127
Final *R*(*F*) [$I > 2\sigma$][a]	0.0771	0.0360	0.0433
w*R*(F_2) indices [I > 2σ]	0.1788	0.0820	0.1172

[a] $R\ (F_o) = \Sigma||F_o| - |F_c||/\Sigma|F_o|$ and $wR(F_o^2) = [\Sigma w(F_o^2 - F_c^2)^2/\Sigma w(F_c^2)^2]^{1/2}$.

(300 MHz, CD_3CN/CD_3OD (1:1), 25 °C): δ = 307 ppm. ESI-MS: 1117 [M], 972 [M – PF_6], 827 [M – 2 PF_6]. $C_{36}H_{46}N_6Se_2PdP_2F_{12}$ (1117.1): calcd. C 38.71, H 4.151, N 7.52; found C 38.95, H 3.81, N 6.56.

$[Pd_2C_{36}H_{46}N_6Se_2P_2F_{12}Cl_2]$ (15): The complex was prepared in a manner similar to that described for **14** and was separated as a yellowish white powder. Yield: 0.18 g, 34%. M.p. 230 °C (d.). IR (KBr): $\tilde{\nu}_{max}$ = 3409 (br), 3205 (w), 1625 (w), 1441 (s), 840 (s), 758 (s), 558 (s) cm^{-1}. ESI-MS: 1148.96 [M – PF_6], 1112.95 [M – (PF_6 + Cl)], 1075.95 [M – (PF_6 + 2 Cl)], 966.95, 928.98 [M – 2 (PF_6 + Cl)], 825.07 [M – (2 PF_6 + 2 Cl + Pd)]. $C_{36}H_{46}N_6Se_2Pd_2P_2F_{12}Cl_2$ (1294.4): calcd. C 33.41, H 3.58, N 6.49; found C 32.72, H 3.44, N 6.52.

X-ray Crystallography: The diffraction measurements for the ligand as well as for the complexes were performed at room temperature on a Bruker P4 diffractometer with graphite-monochromated Mo-K_α radiation (λ = 0.71073 Å) (Table 7 and Table 8) The data were corrected for Lorentz, polarization, and absorption effects The structures were determined by routine heavy-atom with SHELXS 97[25] and Fourier methods, and were refined by full-matrix least-squares by means of the SHELEXL 97[26] program with anisotropic non-hydrogen atoms and a fixed isotropic thermal parameter of 0.07 $Å^2$ for hydrogen. The hydrogen atoms were partially located from difference electron-density maps and the rest were fixed at predetermined positions. Scattering factors were obtained from common sources.[27] Some details of the data collection and refinement are given in Table 8 and Table 9. CCDC-221526 (**11**), -221527 (**8**), -241757 (**4**), -241758 (**7**), -241759 (**9**), -241760 (**10**), and -241761 (**14**) contain the supplementary data for this paper. These data can be obtained free of charge from The Cambridge Crystallographic Data Centre via www.ccdc.cam.ac/uk/data_request/cif.

Acknowledgments

We are grateful to the Department of Science and Technology (DST), New Delhi for funding this work. Additional help from the Regional Sophisticated Instrumentation center (RSIC), Indian Institute of Technology (IIT), Bombay, for 300 MHz NMR spectroscopy, RSIC, CDRI Lucknow, for the mass recording facility, and Tata Institute of Fundamental Research (TIFR), Bombay, for 500 MHz NMR spectroscopy is gratefully acknowledged.

[1] a) K. Gloe, H. Graubaum, M. Wust, T. Rambusch, W. Seichter, *Coord. Chem. Rev.* **2001**, *222*, 103–126; b) J. P. Danks, N. R. Champness, M. Schröder, *Coord. Chem. Rev.* **1998**, *174*, 417–468; c) A. J. Pearson, W. Xiao, *J. Org. Chem.* **2003**, *68*, 2161–2166; d) L. F. Lindoy, in *Progress in Macrocycle Chemistry* (Eds.: R. M. Izatt, J. J. Christensen), John Wiley & Sons, New York, **1987**, vol. 3, ch. 2; e) T. Tsuchiya, T. Shimizu, K. Hirabayashi, N. Kamigata, *J. Org. Chem.* **2003**, *68*, 3480–3485.

[2] a) A. J. Barton, N. J. Hill, W. Levason, G. Reid, *J. Am. Chem. Soc.* **2001**, *123*, 11801–11802; b) W. Levason, G. Reid, *J. Chem. Soc. Dalton Trans.* **2001**, 2953–2960; c) N. J. Hill, W. Levason, G. Reid, *Inorg. Chem.* **2002**, *41*, 2070–2076; d) R. Pietschnig, S. Schaefer, K. Merz, *Org. Lett.* **2003**, *5*, 1867–1869; e) N. J. Hill, W. Levason, R. Patel, G. Reid, M. Webster, *Dalton Trans.* **2004**, 980–981.

[3] a) E. G. Hope, W. Levason, *Coord. Chem. Rev.* **1993**, *122*, 109–170 and references cited therein; b) W. Levason, S. D. Orchard, G. Reid, *Coord. Chem. Rev.* **2002**, *225*, 159–199 and references cited therein; c) A. K. Singh, S. Sharma, *Coord. Chem. Rev.* **2000**, *209*, 49–98 and references cited therein; d) W. Levason, G. Reid, *Comprehensive Coordination Chemistry II* (Eds.: J. A. McCleverty, T. J. Meyer), Elsevier Science, **2004**, *1*, 399 and references cited therein.

[4] a) K. Kobayashi, H. Izawa, K. Yamaguchi, E. Horn, N. Furukawa, *Chem. Commun.* **2001**, 1428–1429; b) J. L. Li, J. B. Meng, Y. M. Wang, J. T. Wang, T. Matsuura, *J. Chem. Soc., Perkin Trans. 1* **2001**, 1140–1146; c) S. K. Tripathi, B. L. Khandelwal, S. K. Gupta, *Phosphorus Sulfur Silicon Relat. Elem.* **2002**, *177*, 2285–2293; d) X. Zeng, X. Han, L. Chen, Q. Li, F. Xu, X. He, Z. Zhang, *Tetrahedron Lett.* **2002**, *43*, 131–134; e) M. J. Hesford, W. Levason, M. L. Matthews, S. D. Orchard, G. Reid, *Dalton Trans.* **2003**, 2434–2442; f) M. J. Hesford, W. Levason, M. L. Matthews, G. Reid, *Dalton Trans.* **2003**, 2852–2858; g) C. Bornet, R. Amardeil, P. Meunier, J. C. Daran, *J. Chem. Soc., Dalton Trans.* **1999**, 1039–1040; h) W. Levason, M. Matthews, R. Patel, G. Reid, M. Webster, *New J. Chem.* **2003**, *27*, 1784–1788.

[5] a) S. C. Menon, H. B. Singh, R. P. Patel, S. K. Kulshreshtha, *J. Chem. Soc., Dalton Trans.* **1996**, 1203; b) S. C. Menon, A. Panda, H. B. Singh, R. J. Butcher, *Chem. Commun.* **2001**, 143; c) S. C. Menon, A. Panda, H. B. Singh, R. P. Patel, S. K. Kulshreshtha, W. L. Darby, R. J. Butcher, *J. Organomet. Chem.* **2004**, *689*, 1452–1463.

[6] a) A. Panda, S. C. Menon, H. B. Singh, R. J. Butcher, *J. Organomet. Chem.* **2001**, *623*, 87–94; b) S. Panda, H. B. Singh, R. J. Butcher, *Inorg. Chem.* **2004**, *43*, 8532–8537.

[7] A. Panda, S. C. Menon, H. B. Singh, C. P. Morley, R. Bachman, T. M. Cocker, R. J. Butcher, *Eur. J. Inorg. Chem.* **2005**, 1114–1126.

[8] S. Panda, H. B. Singh, R. J. Butcher, *Chem. Commun.* **2004**, 322–323.

[9] a) L. Sacconi, F. Mani, A. Benicicni, *Comprehensive Coordination Chemistry* (Eds.: G. Wilkinson, R. D. Gillard, J. A. McCleverty), Pergamon, **1987**, *5*, 55; b) M. Schröder, *Encyclopedia of Inorganic Chemistry* (Ed.: R. B. King), Wiley, New York, **1994**, *5*, 2395.

[10] P. B. Ayscough, *Electron Spin Resonance Chemistry*, Methuen and Co Ltd., **1967**.

[11] S. Brooker, P. D. Croucher, T. N. Davidson, G. S. Dunbar, A. J. McQuillan, G. B. Jameson, *Chem. Commun.* **1998**, 2131–2132.

[12] M. K. Davies, W. Levason, G. Reid, *J. Chem. Soc., Dalton Trans.* **1998**, 2185–2190.

[13] G. Hunter, A. McAuley, T. W. Whitecombe, *Inorg. Chem.* **1988**, *27*, 2634–2639.

[14] J. E. Huheey, E. A. Keiter, R. L. Keiter, in *Inorganic Chemistry: Principles of Structure and Reactivity* 4th ed., HarperCollins College Publishers, New York, **1993**.

[15] M. C. Janzen, M. C. Jennings, R. J. Puddephatt, *Can. J. Chem.* **2002**, *80*, 41–45.

[16] C. M. Bates, P. K. Khanna, C. P. Morley, M. D. Vaira, *Chem. Commun.* **1997**, 913–914.

[17] K.-T. Aye, J. J. Vittal, R. J. Puddephatt, *J. Chem. Soc., Dalton Trans.* **1993**, 1835–1840.

[18] a) W. Levason, J. J. Quirk, G. Reid, C. S. Frampton, *Inorg. Chem.* **1994**, *33*, 6120–6122; b) N. R. Champness, P. F. Kelly, W. Levason, G. Reid, A. M. Z. Slawin, D. J. Williams, *Inorg. Chem.* **1995**, *34*, 651–657; c) N. R. Champness, W. Levason, J. J. Quirk, G. Reid, *Polyhedron* **1995**, *14*, 2753–2758; d) R. J. Batchelor, F. W. B. Einstein, I. D. Gay, J. Gu, B. M. Pinto, X. Zhou, *Inorg. Chem.* **1996**, *35*, 3667–3674.

[19] G. K. Anderson, *Platinum-Carbon σ-bonded Complexes, in Comprehensive Organometallic Chemistry II*. (Eds.: E. W. Abel, F. G. A. Stone, G. Wilkinson), Pergamon, Oxford, **1995**, vol. 9.

[20] a) B. J. Hathaway, A. A. G. Tomilinson, *Coord. Chem. Rev.* **1970**, *5*, 1–43; b) B. J. Hathaway, D. E. Billing, *Coord. Chem. Rev.* **1970**, *5*, 143–207.

[21] C. Beguin, P. Chautemps, A. E. Marzouki, J. L. Pierre, S. M. Refaif, G. Serratrice, E. Saint-Aman, P. Rey, *J. Chem. Soc., Dalton Trans.* **1995**, 1939–1946.

[22] C. Bazicalupi, A. Benicini, S. Ciattini, C. Giorgi, A. Masotti, P. Paoletti, B. Valtoancoli, N. Navon, D. Meyerstain, *J. Chem. Soc., Dalton Trans.* **2000**, 2383–2392.
[23] W. L. F. Armarego, D. D. Perrin, in *Purification of Laboratory Chemicals*, Butterworth-Heinemann, The Bath Press, Bath, **1997**.
[24] a) G. K. Anderson, M. Lin, A. Sen, E. Gertz, *Inorg. Synth.* **1990**, *28*, 60; b) M. G. Simmons, C. L. Merril, L. J. Wilson, L. M. Bottoley, K. M. Kadish, *J. Chem. Soc., Dalton Trans.* **1980**, 1827–1837; c) D. Drew, J. R. Doyle, *Inorg. Synth.* **1972**, *13*, 47.
[25] G. M. Sheldrick, *SHELXS 97, Program for the Solution of Crystal Structures* University of Göttingen, **1990**.
[26] G. M. Sheldrick, *SHELXL 97, Program for Refining Crystal Structures* University of Göttingen, **1997**.
[27] International Tables for X-ray Crystallography, Birmingham, **1974**, 1, 99, 149.

Received: May 9, 2005
Published Online: November 15, 2005

